Human Molecular Genetics, 2019, Vol. 28, No. 4 639–649

doi: 10.1093/hmg/ddy374
Advance Access Publication Date: 24 October 2018
General Article

GENERAL ARTICLE

A variant in *MRPS14* (uS14m) causes perinatal hypertrophic cardiomyopathy with neonatal lactic acidosis, growth retardation, dysmorphic features and neurological involvement

Christopher B. Jackson[1], Martina Huemer[2,3], Ramona Bolognini[4], Franck Martin[5], Gabor Szinnai[3,6], Birgit C. Donner[7], Uwe Richter[8], Brendan J. Battersby[8], Jean-Marc Nuoffer[9,10], Anu Suomalainen[1,11] and André Schaller[4,*]

[1]Research Programs Unit, Molecular Neurology, Biomedicum Helsinki, University of Helsinki, Helsinki FIN-00290, Finland, [2]Division of Metabolism and Children's Research Center, University Children's Hospital Zürich, Zürich CH-8032, Switzerland, [3]University Children's Hospital Basel, University of Basel, Switzerland, [4]Division of Human Genetics, Department of Pediatrics, Inselspital, Bern University Hospital, University of Bern, Bern CH-3010, Switzerland, [5]CNRS, Architecture et Réactivité de l'ARN, Université de Strasbourg, UPR 9002, Strasbourg F-67000, France, [6]Division of Pediatric Endocrinology, University Children's Hospital Basel, Basel CH-4056, Switzerland, [7]Division of Cardiology, University of Basel, Basel CH-4056, Switzerland, [8]Institute of Biotechnology, University of Helsinki, Helsinki, FIN-00014, Finland, [9]Institute of Clinical Chemistry, University of Bern, Inselspital, Bern CH-3010, Switzerland, [10]Division of Endocrinology Diabetology and Metabolism, University Children's Hospital, University of Bern, Bern CH-3010, Switzerland and [11]Neuroscience Center, University of Helsinki, Helsinki FIN-00290, Finland

*To whom correspondence should be addressed at: Division of Human Genetics, Department of Pediatrics, University Hospital Bern, Freiburgstrasse 15, 3010 Bern, Switzerland. Tel: +41 316327845; Fax: +41 316329484; Email: andre.schaller@insel.ch

Abstract

Dysfunction of mitochondrial translation is an increasingly important molecular cause of human disease, but structural defects of mitochondrial ribosomal subunits are rare. We used next-generation sequencing to identify a homozygous variant in the mitochondrial small ribosomal protein 14 (*MRPS14*, uS14m) in a patient manifesting with perinatal hypertrophic cardiomyopathy, growth retardation, muscle hypotonia, elevated lactate, dysmorphy and mental retardation. In skeletal muscle and fibroblasts from the patient, there was biochemical deficiency in complex IV of the respiratory chain. In fibroblasts, mitochondrial translation was impaired, and ectopic expression of a wild-type *MRPS14* cDNA functionally complemented this defect. Surprisingly, the mutant uS14m was stable and did not affect assembly of the small ribosomal subunit. Instead, structural modeling of the uS14m mutation predicted a disruption to the ribosomal mRNA channel.

Received: August 28, 2018. **Revised:** October 12, 2018. **Accepted:** October 16, 2018

Collectively, our data demonstrate pathogenic mutations in *MRPS14* can manifest as a perinatal-onset mitochondrial hypertrophic cardiomyopathy with a novel molecular pathogenic mechanism that impairs the function of mitochondrial ribosomes during translation elongation or mitochondrial mRNA recruitment rather than assembly.

Introduction

Mitochondria contain their own genome and retain an intrinsic bacteriophage/bacteria-like replication and translation machinery. Thirteen proteins need to be expressed from the mitochondrial genome (mtDNA) to produce a functional respiratory system and ATP synthase for oxidative phosphorylation. Over the last decade, genetic mutations that disrupt the function of mitochondrial protein synthesis have been identified with human disease. Surprisingly, very few of these mutations have been identified in the 82 structural subunits of the mitochondrial small and large ribosomal subunits (1). Defects in mitochondrial translation lead to an exceptionally wide range of clinical phenotypes. Most affected individuals show severe early-onset clinical presentations, often with a fatal outcome (2). These gene defects cause typically either a combined deficiency of respiratory chain or an isolated complex IV defect, manifesting in multiple organs or in a tissue-specific manner (3). Currently, the molecular basis by which oxidative phosphorylation defects can manifest with such exceptional clinical heterogeneity cannot be explained.

The human mitochondrial ribosome is a 55S particle, composed of two subunits, a small 28S and a large 39S subunit. The small mitochondrial ribosomal subunit (SSU) is composed of a 12S ribosomal RNA molecule (rRNA) and 30 nuclear-encoded mitochondrial ribosomal proteins (MRPs), whereas the large subunit (LSU) includes 16S rRNA and 52 nuclear-encoded MRPs and either $tRNA^{Phe}$ or $tRNA^{Val}$ (4–7). Both rRNAs, essential for ribosomal integrity and function, are encoded by the mitochondrial genome. Many of the protein subunits of the mitochondrial ribosome (mitoribosome) share structural homology with bacterial counterparts, but 35 out of the 80 MRPs do not and are specific to mammalian mitoribosomes acquired during mitochondrial evolution of mitochondrial gene expression (8,9). Despite recent advances in understanding mitoribosomal structure, the functions of the individual subunits in protein synthesis are still poorly known (4,10).

Here we report that a variant in *MRPS14*, encoding MRPS14, is a novel cause for progressive infantile mental retardation, cachexia, muscular hypotonia, hypertrophic cardiomyopathy, elevated lactate and a complex IV deficiency. Furthermore, we present biochemical and protein modeling data providing information of MRPS14 roles on the mitoribosome.

Results

Patient history

The female proband was the first living child from distantly related Turkish parents. The mother suffered from recurrent depressive episodes. The father had experienced a single episode of rhabdomyolysis followed by undulating plasma creatine phosphokinase (CK) values despite complete clinical restitution. The mother had two spontaneous abortions between gestational weeks 10 and 12. A third pregnancy had been terminated at gestational week 24 due to severe hypertrophic non-compaction cardiomyopathy and intrauterine growth retardation of the female fetus. The index patient was delivered through caesarean section after premature rupture of the membranes at 35 weeks of gestation. The low birth weight (1460 g; <3rd percentile) was attributed to placental insufficiency. Apgar score was 3/6/8 at 1/5/10 min, and the child was admitted to the neonatal intensive care unit due to respiratory insufficiency. Hypertrophic cardiomyopathy, suspected already in the prenatal ultrasound examination, with moderate hypertrophy of the left ventricle and mildly impaired contractility was diagnosed.

Metabolic workup revealed moderately elevated serum lactate (5–7 mmol/L, normal range < 2 mmol/L) and alanine. Organic acids, acylcarnitines, free carnitine, liver transaminases, ammonia, creatinine, complete blood cell counts and creatinine phosphokinase were repeatedly normal. At 4 months, the child was admitted to hospital following an acute life-threatening event at home, which was attributed to severe gastroesophageal reflux. Lactate was again slightly elevated. Cardiologic workup revealed Wolff–Parkinson–White syndrome with an average heart rate of 140/min. Clinical assessment proved generalized muscular hypotonia, failure to thrive and retardation of cognitive and motor development; the electroencephalography was normal.

Respiratory chain (RC) enzyme activity analysis of the patient's skeletal muscle sample revealed mitochondrial complex IV deficiency, reduced to 44% of the controls' mean, whereas the other RC complexes were not affected (Supplementary Material, Fig. S1). Supportive treatment with carnitine, riboflavin, thiamine, vitamin C and coenzyme Q was applied for some months without perceivable positive response. Despite hypercaloric diet, the patient showed failure to thrive. During viral infections or episodes of fever, the child repeatedly experienced acute deterioration, with elevated lactate, metabolic acidosis and poor condition. However, from the age of 2 years onwards, the patient's clinical condition stabilized, and she started to catch up in growth. Her psychomotor development improved, and she learned to walk and talk at the age of 3.5 years. The hypertrophic cardiomyopathy remained stable and caused no clinical problems; episodes of supraventricular tachycardia were not observed.

Presently, at the age of 5 years, the patient walks broad-based, unassisted. She has some dysmorphic features including retroverted low set ears (Fig. 1A). She still has muscular hypotonia, however, less prominent. Her language skills are continuously improving, although not reaching the standard of the age. With five feedings of wholesome food, supplemented with hypercaloric drinks, her weight gain and her growth are now parallel to the 3rd percentile. Her electrocardiography reveals a preexcitation pattern without supraventricular tachycardia, and 3D speckle tracking shows mild segmental dyskinesia in the basal inferior lateral and lateral regions, consistent with an accessory bundle in the lateral wall of the left ventricle. Echocardiography shows no structural abnormalities, and the cardiomyopathy has completely receded. Other functional parameters, including 3D volumetry and strain analysis, are in normal limits. The tissue and pulse wave Doppler measurements show normal diastolic function.

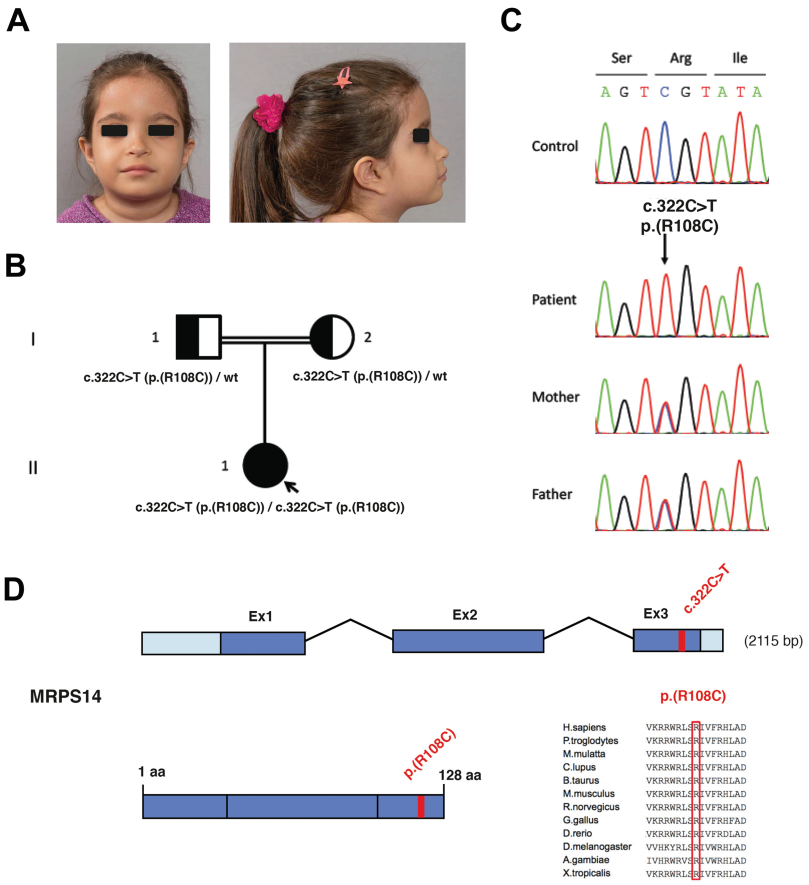

Figure 1. Index patient and targeted sequencing reveals mutations in *MRPS14*. (**A**) Index patient shows discrete facial features of hypertelorism, flat nasal bridge, a small midface region with retroverted and low set ears. (**B**) Pedigree. Index patient (arrow) was born to consanguineous parents. Unaffected heterozygous carriers of the mutant allele are indicated by the half black symbols, and the affected individual is indicated by the solid black symbol. (**C**) Electropherograms show the confirmation of the homozygous c.322C>T in exon 3 of *MRPS14* by Sanger sequencing predicting a p.(Arg108Cys) change. Sanger sequencing was performed in the index patient and its parents, who were both heterozygous carriers. Both parents are clinically unaffected carriers of the same heterozygous variant c.322C>T in *MRPS14*, whereas the clinically affected index patient is homozygous for the c.322C>T variant. (**D**) *MRPS14* mutation analysis shows conservation among different species. Indicated with the arrow is the amino acid change arginine to cysteine at position 108 resulting from the c.322C>T transition.

Next-generation MitoExome sequencing revealed a recessive homozygous *MRPS14* mutation in the patient

We utilized next-generation MitoExome sequencing for molecular genetic investigations (11). The targeted MitoExome approach analyzed sequences of 1476 nuclear genes encoding proteins with mitochondria-associated functions. Data analysis led to the identification of a homozygous variant in *MRPS14* (NM_022100), c.322C>T (Combined Annotation Dependent Depletion (CADD) score 8.03) in exon 3 (Fig. 1B and C). *MRPS14* was the only candidate gene fitting a recessive homozygous trait considering the parental consanguinity. This variant was not reported in any database (ExAC, gnomAD) (12). The functional impact of the c.322C>T transition has eight pathogentic computational verdicts (DANN, GERP, LRT, MetaLR, MetaSVM, MutationAssessor, MutationTaster and PROVEAN [listed in (13)]). Confirmation of the variant was performed by Sanger sequencing. Carrier analysis showed that both the parents were heterozygous carriers for the c.322C>T variant (Fig. 1C). Human *MRPS14* encodes a 128 amino acid long protein that is a structural component of the mitoribosome SSU. The c.322C>T variant is predicted to alter a highly conserved arginine to a cysteine at position 108 in uS14m (Fig. 1D). Collectively, our data are consistent with the c.322C>T *MRPS14* variant as the underlying pathogenic cause of the patient's clinical presentation.

Decreased mitochondrial respiration and multiple respiratory chain complex deficiency in patient fibroblasts

Next, we analyzed the patient's fibroblasts to test whether the c.322C>T variant was pathogenic and disrupted mitochondrial protein synthesis. Blue-native gel electrophoresis analysis of the native respiratory complexes revealed combined deficiency of assembled oxidative phosphorylation complexes, with CI and CIV barely detectable and CIII and CV markedly decreased (Fig. 2A). Steady-state mitochondrial respiratory proteins showed decreased levels of respiratory complex subunits with most substantial decrease in subunits probed for complex I and IV (Fig. 2B). The exclusively nuclear-encoded complex II showed no significant reduction compared with controls (Fig. 2B). These changes of multiple respiratory chain deficiency were also reflected in base-level oxygen consumption, with a markedly deficient ADP-dependent and slightly decreased

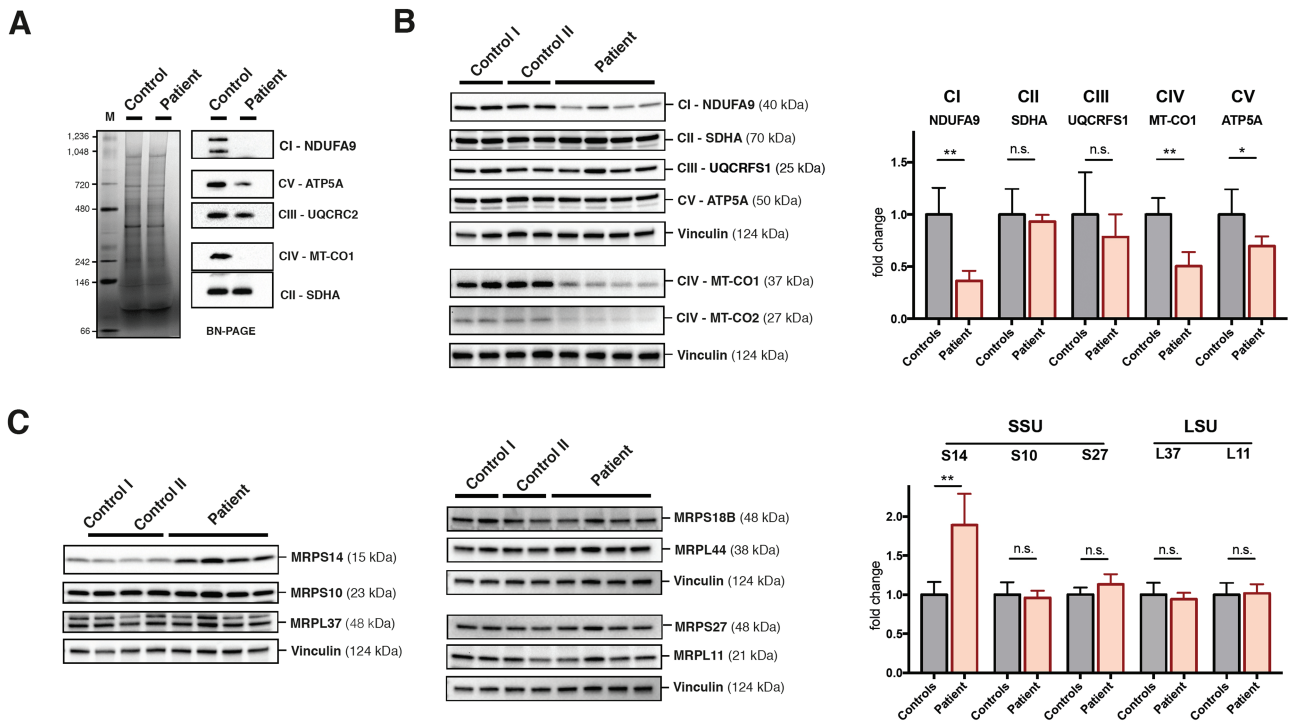

Figure 2. *MRPS14* mutated fibroblasts present with multiple respiratory complex deficiencies. (**A**) Immunoblot of blue-native respiratory chain complex analysis from total cell lysates of control and patient cells. Patient's cells show drastically reduced assembled complex I, IV and V, reduced complex III with unchanged complex II. (**B**) Immunoblots of steady-state mitochondrial respiratory chain complex subunits reveals multiple complex deficiencies in patient's fibroblasts with significant reduction of CI, CIV and CV. Graph represents immunoblot quantification of average of groups with standard deviation. Vinculin was used as loading control for normalization. (**C**) Immunoblots of steady-state MRPs of the small (SSU: MRPS10, MRPS18B, MRPS27) and large (LSU: MRPL11, MRPL37, MRPL44) subunit remain unchanged apart from a 2-fold increase in uS14m in patient's cells. Graph represents immunoblot quantification of average of groups with standard deviation. Vinculin was used as loading control for normalization. Controls represent fibroblast lines derived from healthy individuals in two biological replicates (subculturings); patient represents four biological replicates (subculturings). Unpaired *t*-test, statistical significance: n.s. (not significant), $^{*}P \leq 0.05$, $^{**}P \leq 0.01$.

complex IV-dependent respiration activity (Supplementary Material, Fig. S2A) and partially distorted mitochondrial structure (Supplementary Material, Fig. S2B) but no changes in mitochondrial mass in patient cells compared with controls (Supplementary Material, Fig. S2C). Confirming mitochondrial disease etiology, we probed for steady-state levels of mitochondrial small (SSU) and large (LSU) ribosomal subunits to assess ribosomal integrity. Intriguingly, when we assessed the steady-state levels of mitochondrial small (SSU) and large (LSU) ribosomal subunits, we found MRPS14 levels were increased in the patient, whereas all SSU (MRPS10, MRPS18B, MRPS27) and LSU (MRPL11, MRPL37, MRPL44) subunits tested remained unchanged compared with controls (Fig. 2C), indicating that the c.322C>T variant in *MRPS14* does not impair the assembly of the SSU.

The c.322C>T variant in *MRPS14* does not affect ribosome assembly or 12S rRNA stability but is essential for mitochondrial translation

To assess the assembly status of the entire mitoribosome and to confirm insertion of MRPS14 into the SSU, sucrose gradients analysis was performed. Probing against MRPS18B revealed specific and comparable separation of mitoribosomal components in control and patient's fibroblasts (Fig. 3A). MRPS14 was found both in the SSU and monosome fractions comparable to controls, suggestive of insertion of both wild-type (WT) and mutant protein (Fig. 3A). Probing of LSU subunit MRPS27 and LSU subunits MRPL23 and MRPL44 was unchanged compared with patients, demonstrating the mitoribosome to be intact in the patient's cells.

Northern analysis of the steady-state mtDNA transcript levels showed no reduction in the 12S rRNA compared with controls, which would indicate instability or assembly deficiency of the SSU (Fig. 3B, quantification Supplementary Material, Fig. S3A). LSU-associated 16S rRNA and ATP8/6 mRNA were unchanged relative to total RNA (Fig. 3B; Supplementary Material, Fig. S3A). These findings were corroborated by quantitative PCR (Fig. 3C). The comparable amount of 12S rRNA supported the conclusion that the mutated MRPS14 did not impair assembly or stability of the SSU. However, the role of MRPS14 in the assembly or stability of the small mitoribosomal subunit and effect on translation of specific mRNAs is unknown. Up to date, mutations reported in mitochondrial ribosomal subunits cause protein instability with subsequent instability or defective assembly of the mitoribosome and its associated rRNAs (14–20). Western blot analysis indicated that the mutant MRPS14 protein was stable, suggesting it to be inserted into the mitoribosome and directly interfere with the mitochondrial translation process rather than affect mitoribosome assembly or stability (Fig. 2C).

To directly test whether the c.322C>T variant in *MRPS14* indeed impaired the mitochondrial translation; we labeled the mitochondrial translation products in the fibroblasts by metabolic ^{35}S-labelling. Pulse-labelling revealed a general mitochondrial translation defect in the patient's fibroblasts compared with the controls as total [^{35}S]-met/cys incorporation was significantly reduced (Fig. 3D and E). Due to apparent

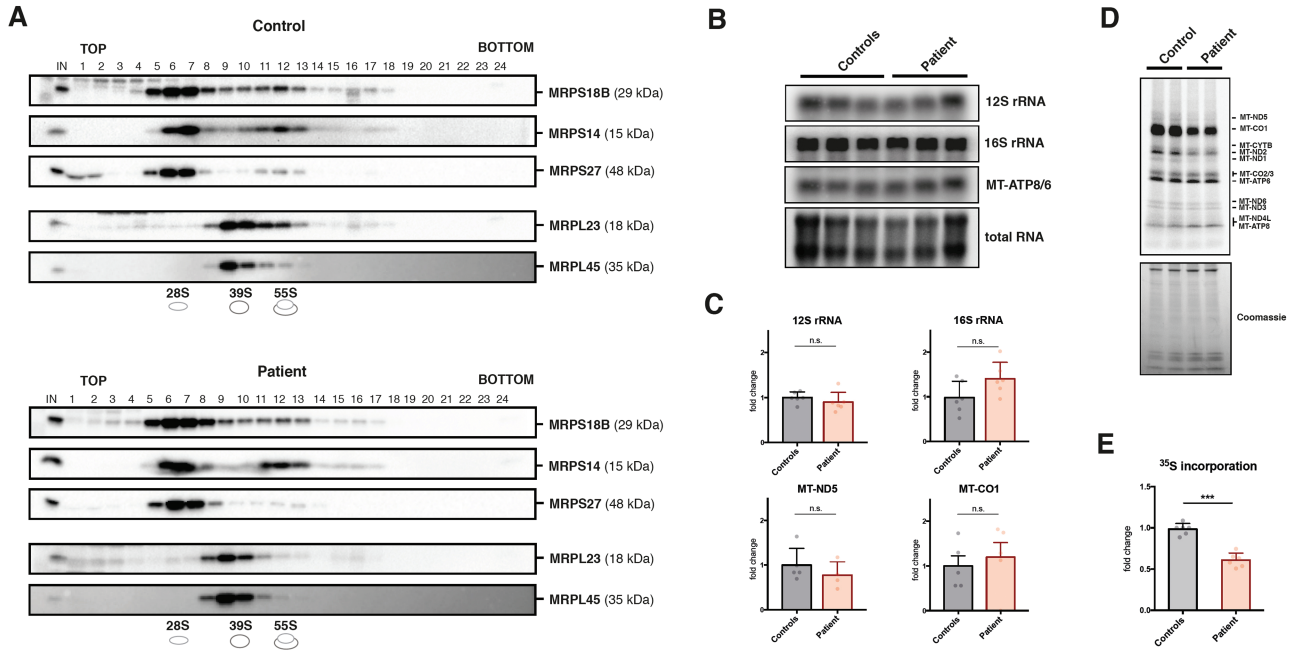

Figure 3. Mitochondrial translation capacity and ribosome assembly state in patient fibroblasts. (**A**) Immunoblotting of fractions from linear 10–30% sucrose density gradients of control and patient's fibroblasts. Probing against SSU subunits uS14m, MRPS27 and MRPS18B reveal an equal distribution of 28S to fully assembled 55S between control and patient with no particular assembly intermediates or gross assembly defect in the patient. A fraction of input for the sucrose gradient was used as control (IN). Numbers indicate respective fractions collected from top to bottom. (**B**) Northern blot analysis of total RNA from control ($n = 3$) and patient's cells from three subculturings for 12S and 16S rRNAs and MT-ATP6/8 transcript reveal no significant changes in the patient (quantification, Supplementary Material, Fig. S3A). (**C**) Quantitative PCR of mitochondrial transcripts (12S rRNA, 16S rRNA, MT-ND5, MT-CO1) in controls and patient's cells reveal no significant changes in 12S rRNA and replicate northern blot findings. Controls represent three fibroblast lines derived from healthy individuals; patient represents four biological replicates (subculturings). Graph represents group average (with duplicate runs for 12S and 16S rRNA). β-actin was used for normalization. (**D**) ^{35}S-metabolic labelling reveals a general decrease in mitochondrial translation in patient's fibroblasts (30 min pulse). Coomassie staining was performed as loading control. (**E**) Quantification of ^{35}S-met/cys incorporation in patient relative to control from three independent experiments performed in biological duplicates. Graph represents quantification of ^{35}S incorporation of average of groups with standard deviation. Coomassie was used as loading control for normalization. Unpaired *t*-test, statistical significance: n.s. (not significant), $^{*}P \leq 0.05$, $^{**}P \leq 0.01$, $^{***}P \leq 0.001$.

stability of the mitoribosome, we performed a chase experiment to exclude a specific translational interaction or modification to any mitochondrially translated protein resulting in increased instability, which did, however, not show any complete turnover of a specific product (Supplementary Material, Fig. S3B). Silencing of MRPS14 did not result in a lower steady-state level of MT-CO1, suggesting that the residual amount of wild-type (WT) mitoribosomes was enough to maintain its levels (Supplementary Material, Fig. S4). In conclusion, these results indicate that the *MRPS14* variant severely inhibits translation efficiency in the patient's fibroblasts without affecting general SSU assembly, the—reported late stage (21)—addition of MRPS14 to the SSU itself or 55S monosome assembly.

Modelling the putative role of MRPS14 (uS14m) on 55S ribosome

Recent high resolution cryo-electron microscopy (EM) structure of the human mitoribosome initiation complex (22) allowed us to investigate the putative structural impact of the R108C mutation. This structure is especially interesting because it allowed a careful assessment of the position of this residue and its integration into the translation initiation complex containing a tRNA and mRNA (4,23). uS14m is part of the head of the SSU forming a cluster with MRPS24 and uS10m similar to the bacterial counterpart (with the exception of bS6m and uS12m). Mitochondrial specific N-terminal amino extension (NTE) and C-terminal amino acid extension (CTE) are unique features of 15 of the 31 SSU subunits (with the exception of bS6m and uS12m), which are homologous to their bacterial counterpart. They are of varying length and potentially form solvent interaction sites. The NTE of uS14m is located to the solvent side, as is the NTE and CTE of uS10m. Interestingly, uS14m is located in the mRNA entrance channel on the small ribosomal subunit at the interface with the LSU (Fig. 4A). In this structure, the distance between R108 and the tRNA anticodon is above 30 Å (Fig. 4B). The lateral chain of the amino acid R108 affected in the patient interacts with both the SSU ribosomal protein uS10m on one side and the sugar phosphate backbone of residue A579 of 12S rRNA on the other side (Fig. 4C). Therefore, R108 occupies a key position that links the 12S rRNA to ribosomal protein uS10m. A cysteine at position 108 would be predicted to disrupt both interactions, thereby probably leading to an altered conformation of the mRNA channel or the ribosome decoding center (Fig. 4D). Such a model is consistent with our findings that only mitochondrial translation elongation or mitochondrial mRNA recruitment is disrupted in patient fibroblasts and not the assembly of mitoribosomes.

Wild-type *MRPS14* rescues the respiratory chain deficiency and mitochondrial translation defect in patient cells

To directly test the pathogenicity of the c.322C>T variant in *MRPS14*, we cloned the WT and variant *MRPS14* cDNAs

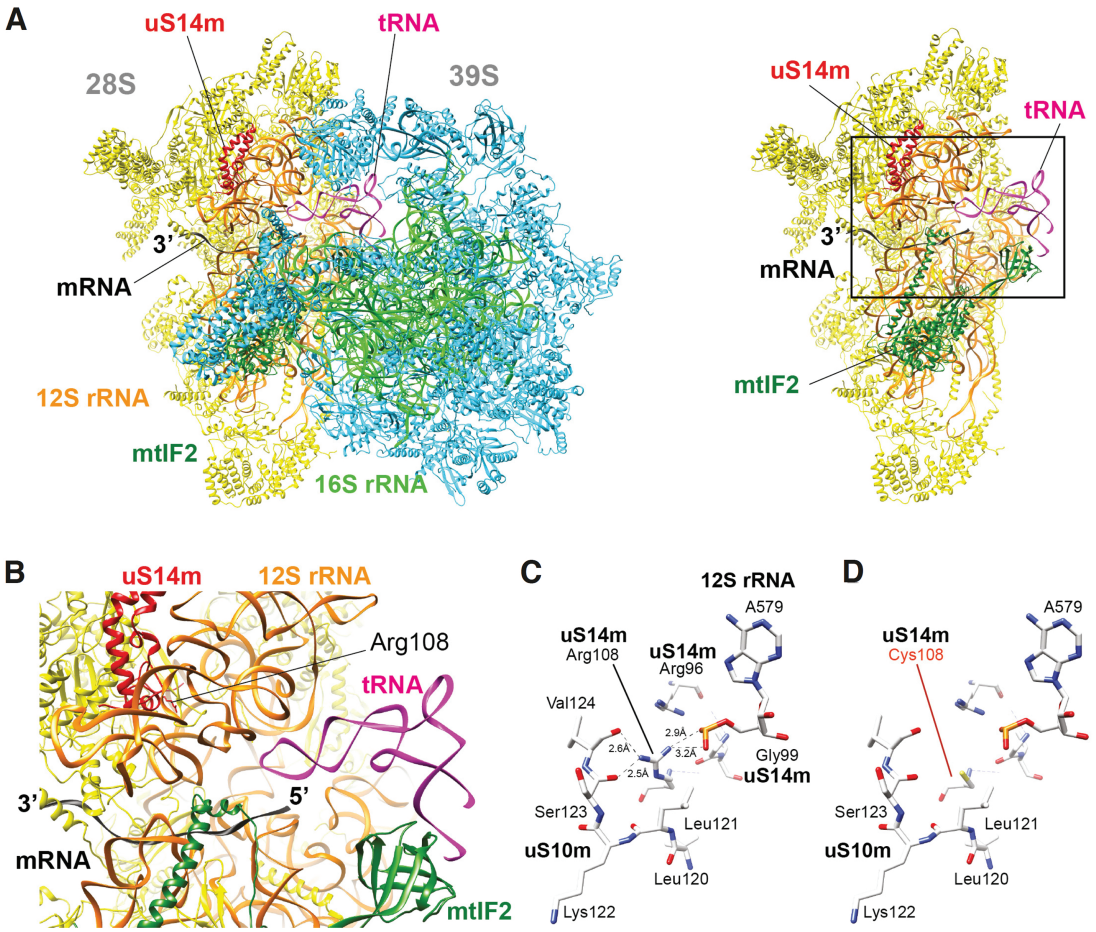

Figure 4. Modelling of uS14m (MRPS14) mutation R108C within the 55S mitochondrial initiating ribosome. **(A)** Human mitochondrial initiating ribosome structure (pdb 6GAW) (4): the ribosomal proteins from the small subunit are shown in yellow, and the 12S rRNA is shown in orange. The ribosomal proteins from the LSU are shown in blue, and the 16S rRNA is shown in green. The mRNA is shown in black, and the tRNA in magenta. The mitochondrial initiation factor mtIF2 is shown in dark green. Ribosomal protein uS14m is shown in red. On the left, the complete structure of the initating 55S ribosome is shown: on the right, the LSU has been removed. The black frame indicates the part of the structure that is magnified and shown in **(B)**. This magnification shows the position of the small ribosomal subunit protein uS14m in red in respect to the tRNA anticodon (in magenta) and the mRNA (in black) in the mRNA channel. The lateral chain of Arg108 is also shown in red. **(C)** Arg108 lateral chain interacts with ribosomal protein uS10m (MRPS10) and the sugar phosphate backbone from A579 of 12S rRNA. **(D)** By modelling, the lateral chain of residue 108 has been replaced by a cysteine lateral chain, thereby illustrating the probable structural consequences of the R108C mutations and the loss of the previously mentioned interactions with ribosomal protein uS10m and 12S rRNA (A579).

to a lentiviral expression system. Both *MRPS14* cDNAs were transduced into the patient's and control's fibroblasts. Overexpression of the WT *MRPS14* cDNA in the patient's fibroblasts complemented the steady-state protein levels of MT-CO1 and MT-CO2 and mitochondrial translation (Fig. 5A). In contrast, overexpressing the mutation in the patient background failed to rescue the defect in mitochondrial protein synthesis (Fig. 5A) Surprisingly, the overexpression of the R108C mutant in control's fibroblasts generated a dominant-negative phenotype, reducing MT-CO1 and MT-CO2 abundance (Fig. 5A). To corroborate these findings, metabolic ^{35}S-pulse-labelling in the same transduced fibroblast lines was performed (Fig. 5B). As suggested by rescued steady-state MT-CO1 and MT-CO2 levels, mitochondrial translation capacity was complemented in patients' cells overexpressing WT with *MRPS14* cDNA (Fig. 5B).

This would suggest the mutant protein was assembled into the ribosome and is critical for mitochondrial protein synthesis. Together, these data support the pathogenicity of the c.322C>T *MRPS14* mutation as the underlying cause of the biochemical defect in oxidative phosphorylation in the patient.

Discussion

Here, we report a novel pathogenic mutation in *MRPS14* that manifests as a perinatal mitochondrial hypertrophic cardiomyopathy. The pathogenic role was supported by (1) segregation in the family, (2) high conservation of the mutation site and modeling-based prediction of severe effects of the mutation in intraribosomal interactions, (3) patient's clinical and cellular phenotype mimicking those of other mitochondrial ribosome defects and (4) functional complementation of the biochemical defects with overexpression of the WT protein. This is the first reported pathogenic mitoribosomal defect not affecting the assembly or stability of the mitoribosome, evidencing that the mitoribosome allows incorporation of mutant proteins and instead, disrupt the function of the mitoribosome during translation elongation or mitochondrial mRNA recruitment.

Approximately 80 ribosomal proteins are assembled into the mitochondrial 55S ribosome, and surprisingly, few have been associated with human diseases or are considered possibly disease-causing (Table 1). This suggests that many potential

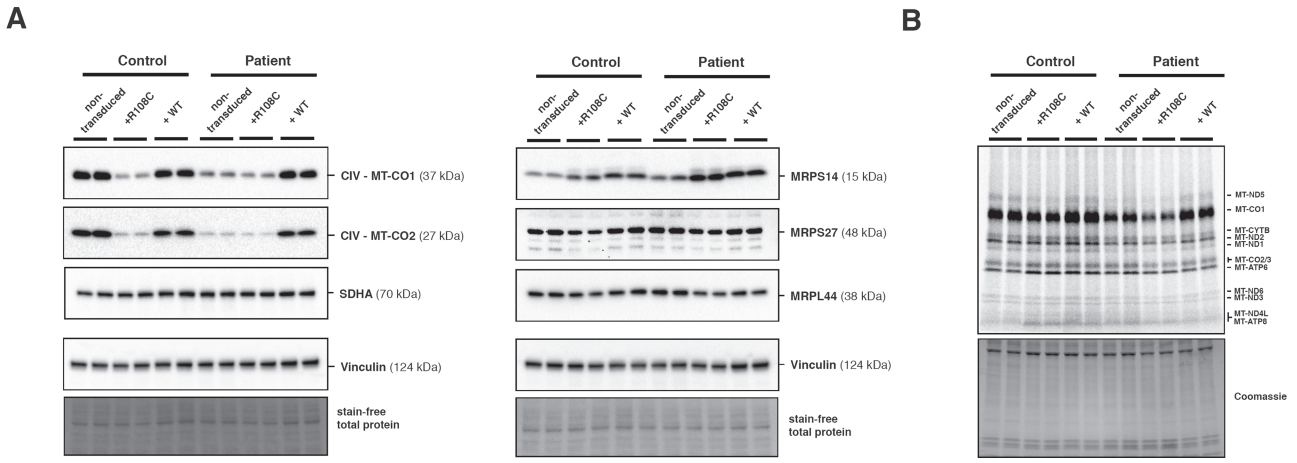

Figure 5. Functional rescue of MRPS14-deficient fibroblasts corrects mitochondrial translation phenotype. **(A)** Immunoblots of steady-state levels of respiratory chain and mitochondrial ribosomal subunit from control and patient's fibroblasts transduced with WT or mutant (+R108C) MRPS14. Patients show reduced steady-state level of MT-CO1 compared with controls (non-transduced cells). Stably transduced clones expressing mutant MRPS14 (+R108C) show decrease steady-state levels of MT-CO1 in both control and patient with additive effect in patient's cells. Transduction with WT MRPS14 rescues MT-CO1 and MT-CO2 levels in patient's fibroblasts, confirming the pathogenicity of the R108C mutation. Expression levels of MRPS14 in stably transduced cells reveal partial overexpression with additive effect in patient cells. Mitochondrial complex II subunit SDHA, mitochondrial ribosomal small (MRPS27) and large (MRPL44) subunits remain seemingly unaffected. Samples are represented in technical duplicates, and Vinculin and stain-free total protein serve as loading control. **(B)** ^{35}S-metabolic labelling of patient cells stably transduced with WT cDNA of MRPS14 show increased translation rates in patient cells and corroborates rescued steady-state MT-CO1/2 levels in (A). Samples are represented in biological duplicates and coomassie serves as laoding control.

Table 1. Disease-associated mitochondrial ribosomal genes

MRPL	Phenotype	Mutation	Reference
MRPL3	HCM, psychomotor retardation	c.950C>G (p.Pro317Arg) /large deletion	(24)
MRPL12	Growth retardation, neurological deterioration	c.542C>T (p.Ala181Val)	(16)
MRPL44	Infantile cardiomyopathy	c.467C>G (p.Leu156Arg)	(20,25)
MRPS			
MRPS2	Hypotonia, hyperlacticacidemia, growth retardation	c.328C>T (p.Arg110Cys) c.340G>A (p.Asp114Asn) c.413G>A (p.Arg138His)	(26)
MRPS7	Hepatic and renal failure, sensorineural deafness	c.550A>G (p.Met184Val)	(19)
MRPS14	**HCM, cachexia, lactic acidosis**	**c.322C>T (p.Arg108Cys)**	**this report**
MRPS16	Fatal lactic acidosis, CM Tubulopathy, hypotonia, skin edema	c.331C>T (p.Arg111*)	(15,17)
MRPS22	CM, tubulopathy, hypotonia, skin edema, Cornelia de Lange-like dysmorphic features, encephalocardiomyopathy	c.509G>A (p.Arg170Cys) c.644T>C (p.Leu215Pro)	(15,18,27,28)
MRPS23	Hepatic disease	c.119C>G (p.Pro40Arg)	(29)
MRPS34	Leigh syndrome, hyperlactic acidemia, microcephaly, transient metabolic acidosis	c.321+1G>T (p.?) c.322-10G>A, (p.?) c.37G>A (p.Glu13Lys), c.94C>T (p.Gln32*)	(14)

Abbreviations: MRPS—MRP SSU, MRPL—MRP LSU, HCM—hypertrophic cardiomyopathy, CM—cardiomyopathy.

mutations are so severe that they result in early embryonic lethality. Consistent with this hypothesis, the presented family had a history of repeated miscarriages. Previously, human disorders have been associated with *MRPS2* (24), *MRPS7* (11), *MRPS16* (12), *MRPS22* (13,14), *MRPS23* (15) and *MRPS34* (14) of the small mitochondrial ribosomal subunit and mutations in *MRPL3* (16), *MRPL12* (17) and *MRPL44* (18) encoding proteins of the large ribosomal subunit. These defects often are associated with neonatal hypertrophic cardiomyopathies, similar to our patient. However, the fetal manifestation in the current patient and her sibling is among the earliest manifestations reported, mimicking that of an alanine tRNA synthetase defect (30).

Clinically, patients with defects of the mitochondrial ribosome often present with hypertrophic cardiomyopathy, which in our patient was accompanied by mental retardation, muscle hypotonia, dysmorphism and neurological features with lactic acidosis. Defects to mitochondrial protein synthesis universally disrupt the synthesis of the 13 mtDNA-encoded subunits required for oxidative phosphorylation and yet, are associated with a broad heterogenous clinical presentation (Table 1). All of the reported cases of mitoribosomal subunit defects manifest early in childhood and are often fatal. However, some can survive beyond the critical infantile years with an apparently stable cardiac phenotype (20). The same natural history is observed in

our patient. The molecular mechanisms by which cardiac tissue might compensate for a severe mitochondrial translation defect remain to be discovered.

Reported defects of the mitochondrial SSU lead to protein instability and cause impaired assembly of the small 28S ribosomal subunit and reduction of 12S rRNA, which is degraded if not incorporated to SSU during assembly (15,17,19,27,31). We found mutant MRPS14 to be stable, strongly supporting insertion of the mutant protein into the mitoribosome, without affecting gross ribosomal assembly or its stability. It is possible, however, that the mutated patient mitoribosome lacks subunits not essential for assembly and not resolved on sucrose gradients. Whether complete ablation of MRPS14 would cause SSU assembly or stability defects is still unknown. Suprisingly, overexpression of mutant MRPS14 protein phenocopied the patient's biochemical findings. Whether the increased steady-state level of MRPS14 in patient's cells is a compensatory effect, however, could not be conclusively addressed nor could the ratio of mutant and WT MRPS14 be determined. We therefore assigned this dominant-additive effect of mutant MRPS14 to its overexpression. Although the heterozygous parents were subclinical, the father presented with a single episode of rhadomyolysis and varying abnormal CK values, suggesting a possible partial dominant negative effect.

Our protein modeling predicted MRPS14 to be located in the mRNA channel, a core functional center of the ribosome, with close contact with both the mRNA and the 12S rRNA. This proposes a possible role for *MRPS14* to contribute to the recruitment and guidance of the leaderless mitochondrial mRNAs to the ribosome and resulting impaired translation efficiency. This function would correspond well with the functional defects detected in the patient's fibroblasts, which were able to produce translation products, but with severely reduced efficiency.

Dysmorphic features are common to mitochondrial disease and are described in other patients with SSU gene mutation but have led to the hypothesis that they have an additional role in development. Furthermore, MRPs have been reported to contribute to apoptosis and regulation of cell proliferation and even associated with neoplasms (32–36). We cannot exclude contribution of such additional functions to the patient's phenotype. However, our data implicate that *MRPS14* is crucial for a highly functional mitochondrial translation machinery and thereby oxidative phosphorylation, two essential functions sufficient to explain the leading clinical manifestations of the patient, including the cardiomyopathy.

We report *MRPS14* as a novel gene causing mitochondrial hypertrophic cardiomyopathy with dysmorphic features and neurologic involvement, with potential cause of a lethal phenotype in affected fetuses.

Materials and Methods

OXPHOS assay

Activity measurements of OXPHOS complexes were performed in mitochondria of skeletal muscle homogenates (supernatants pelleted by centrifugation at 600 xg) as previously studied (37). Individual respiratory chain complex activities and the activity of the citrate synthase (CS) used as marker enzyme were measured spectrophotometrically using a UV-1601 described spectrophotometer (Shimadzu, Hamburg, Germany) in 1 ml sample cuvettes maintained at 30°C according to Birch-Machin (20). Values were determined by measuring the differences of the complex activity levels in the presence and the absence of specific inhibitors, expressed as ratio to the marker enzyme CS (mU/mU CS) as described elsewhere (22). Muscle biopsies of patients without a biochemical and clinical suspicion of a mitochondrial disorder served as a control.

DNA extraction

DNA was extracted from EDTA-blood from the patient and her parents using a Prepito DNA Blood600 Kit according to the manufacturer's instructions (PerkinElmer, Waltham, MA, USA). DNA extracted from EDTA-blood was used as template to produce northern blot probes.

Mitochondrial transcript quantification

RNA from cultured cells was extracted using the Qiagen (Hilden, Germany) miRNA kit including a DNase digestion step. To generate cDNA using Maxima first-strand cDNA synthesis kit (ThermoFisher, Waltham, MA, USA), 2 µg of total RNA was used. Quantitative real-time PCR amplification of cDNA was performed with IQ SybrGreen kit (Biorad, Hercules, CA, USA) on CFX96 Touch qPCR system (Biorad, Hercules, CA, USA). Relative expressions were normalized to β-actin or 18S rRNA. (Primer sequences, Supplementary Material, Table S1).

Library preparation, targeted sequencing and data analysis

Next generation sequencing was performed via a MitoExome panel (11). Briefly, 1 µg genomic DNA was sheared into fragments of about 300 bp using Covaris M220 Focused Ultrasonicator (Covaris, Brigthon, United Kindgom) according to the manufacturer's protocol. Library preparation was performed with the Kapa Library Preparation Kit (Kapa Biosystems, Basel, Switzerland) according to manufacturer's instructions. In solution capturing, (NimbleGen, Roche, Basel, Switzerland) was used to capture the target regions of 1476 genes (MitoExome). A total of 150 bp paired-end sequencing was performed on a HiSeq2000 (Illumina, San Diego, CA, USA). Sequence data analysis was performed using CLC Genomics Workbench v7.0.3 (CLCbio, Qiagen, Hilden, Germany) for read alignment to the human reference genome GRCh38/hg19, local realignment and variant calling. Variants, which were intronic, synonymous, with a coverage <20 and with a minor allele frequency (MAF) of $>1\%$ were excluded, and non-synonymous variants predicted as deleterious (PolyPhen), damaging (SIFT) or with unknown consequences with a MAF of $\leq 1\%$ were retained.

Molecular genetics

Analysis of the prioritized homozygous variant in *MRPS14* was performed by Sanger sequencing. Exon 3 of *MRPS14* (NM_022100) was amplified using genomic DNA as template and was sequenced on an ABI Prism 3500XL Genetic Analyzer (Applied Biosystems, Foster City, CA, USA) using BigDye Terminator v3.1 chemistry (Applied Biosystems, Foster City, CA, USA). Sequence data were analyzed with SeqAnalysis 6 (Applied Biosystems, Foster City, CA, USA) and Sequence pilot v4.3 (JSI Medical Systems, Ettenheim, Germany).

Cell culture

Primary fibroblast cultures derived from a skin biopsy of the patient and control subjects were cultured in DMEM

(1X) + GlutaMAX-I containing 1 g/L D-glucose and 110 mg/L sodium pyruvate (Gibco, Life Technologies, Carlsbad, CA, USA), supplemented with 10% fetal bovine serum (FBS) (Gibco, Life Technologies, Carlsbad, CA, USA), non-essential amino acids (Gibco, Life Technologies, Carlsbad, CA, USA), 50 U/ml penicillin and 50 µg/ml streptomycin (Gibco, Life Technologies, Carlsbad, CA, USA), 10 µg/ml chlortetracycline (Sigma, Helsinki, Finland) and 2 µmol/L uridine at 37°C and 5% CO_2.

RNA isolation and northern blotting

RNA was isolated from primary fibroblasts by using a QIAgen RNeasy Kit (Qiagen, Hilden, Germany) according to the manufacturer's protocol, including an RNase-free DNase digestion step to remove contaminating DNA. Nothern blot analysis has been done as described before (36). Briefly, RNA (10 µg) was separated by a 1.5% denaturing agarose/formaldehyde gel and transferred by capillary transfer in 20X SSC to a 0.45 µm Hybond-N+ nitrocellulose membrane (Amersham, GE Healthcare, Chicago, IL, USA). RNA was covalently bound to the membrane in a UV-crosslinker (UV Stratalinker 1800, Strategene, San Diego, CA, USA) and hybridized. Probes for northern blotting were end-labelled with gamma ATP using PNK according to manufacturer's recommendations. Membranes were stripped in 0.5% SDS at 60°C and stored at 4°C until pre-hybridization.

Cloning and lentiviral-based complementation

Single-stranded cDNA was used as a template to amplify WT and mutant MRPS14 including a *NheI* overhang for cloning. Amplified RT-PCR products were cloned into the lentiviral vector pLVEF1a-MCS-IRES-Puro (Biosettia, San Diego, CA, USA) to obtain pLV-EF1a-wtMRPS14-IRES-Puro and pLV-EF1amutMRPS14-IRES-Puro using the *NheI* site of the MCS and verified by sequencing. Stable lines were produced by selecting transduced fibroblasts with puromycin (1 ug/ml). Transduction was performed following general protocols.

SDS and blue native and protein assay

Total protein was extracted with radioimmunoprecipitation assay (RIPA) buffer using protease, phosphatase inhibitors tablets (ThermoFisher, Waltham, MA, USA) and sodium orthovanadate. Protein concentrations were determined using Bradford assay. Proteins were separated by SDS-PAGE using 4–20% gradient gels and transferred to PVDF membranes. Blots were blocked with 5% [w/v] milk in Tris-buffered saline with 1% [v/v] Tween 20 (TBST) buffer for 1 h, and antibodies were incubated at 4°C overnight at 1:1000 dilution in 1% [w/v] milk in TBST buffer. Antibodies used for western analyses were MT-CO1(ab14705), MT-CO2(ab110258), SDHA(ab14715), ATP5A (ab14748), NDUFA9 (ab14713), UQCRFS1 (ab14746) VDAC (ab15895) Vinculin (ab129002) (all from Abcam, Cambridge, UK), MRPS14 (HPA051087), MRPS10 (HPA029134) (all from Sigma-Aldrich, Helsinki, Finland), MRPS27 (17280-1-AP), MRPS18B (16139-1-AP), MRPL11 (15543-1-AP), MRPL23 (11706-1-AP), MRPL44 (16394-1-AP), MRPL37 (15190-1-AP) (all from Proteintech, Manchester, UK) TOM20 (sc-11415, SantaCruz, Dallas, TX, USA).

Native mitochondrial complexes were prepared from digitonin-solubilized laurylmaltoside-treated fibroblasts as described before (38). Briefly, harvested cells were solubilized in 5 mg/ml digitonin for a 0.8 digitonin to total protein ratio in 1×PBS in the presence of protease inhibitors (ThermoFisher, Waltham, MA, USA). Solubilized cells were then pelleted, resuspended in 1.5 M aminocaproic acid, 75 mM Bis-tris pH 7.0, 10 mM EDTA and treated with 1% [w/v] laurylmaltoside to liberate respiratory complexes. 10–30 ug of mitochondria-enriched protein was separated on 4–16% Bis-Tris gels (Life Technologies, Carlsbad, CA, USA) for 5 h and transferred onto PVDF membranes. Blocked membranes were sequentially incubated overnight with MT-CO1 (ab14705), SDHA (ab14715), ATP5A (ab14748), NDUFA9 (ab14713) and UQCRC2 (ab14745) (all from Abcam, Cambridge, UK) and detected with appropriate secondary-HRP antibodies using chemiluminescence.

Pulse-labelling of mitochondrial translation products

Pulse-labelling was performed as described (36). Briefly, fibroblasts were grown in 35 mm dishes to 60–70% confluency. Growth media was removed and replaced by methionine/cysteine-free medium (Gibco, Life technologies, Carlsbad, CA, USA) supplemented with sodium pyruvate (Gibco, Life technologies, Carlsbad, CA, USA) and pre-incubated before labelling at 37°C for 30 min. Cells were incubated for 6 min in met/cys-free medium supplemented with 10% dialyzed FBS (Gibco, Life technologies, Carlsbad, CA, USA) and 1 mM sodium pyruvate in the presence of 0.5 µg/ml emetine (Sigma, Helsinki, Finland, E2375) or 100 µg/ml anisomycin (Sigma, Helsinki, Finland, A9789) to inhibit cytoplasmic translation prior to the addition of the radiolabel mix. For pulse-labelling, 200 µCi/ml [^{35}S]-met/cys (PerkinElmer, Waltham, MA, USA) was added to the medium and incubated for 30 min. Cells were washed in growth media and 1×PBS before being trypsinized, collected by centrifugation and resuspended in 1×PBS containing 1 mM PMSF (Sigma, Helsinki, Finland) and EDTA-free protease inhibitors (Roche, Basel, Switzerland). For chase labelling, cells were washed after 30 min and incubated in normal growth medium for 3 h after which cells were washed and harvested. Bradford assay was performed to determine protein concentration according to the manufacturer's protocol (Biorad, Hercules, CA, USA). 30 µg of total protein extracts were separated on 12% polyacrylamide gels at 20 mA for 2 h. Gels were stained in Coomassie staining solution (1 g Coomassie brilliant blue in 40% [v/v] methanol, 10% [v/v] glacial acetic acid, 3% [v/v] glycerol and 47% [v/v] H_2O) overnight and destained in destaining solution (40% [v/v] methanol, 10% [v/v] glacial acetic acid, 3% [v/v] glycerol and 47% [v/v] H_2O) for 2 h. Gels were dried using a vacuum gel dryer Model 583 (Biorad, Hercules, CA, USA) for 2 h at 60°C and subsequently exposed to a phosphor screen for at least 24 h. Phosphor imaging screens were imaged using a FLA-7000 Typhoon scanner (GE Healthcare, Chicago, IL, USA), and total protein was imaged using a Chemidoc imaging system (Biorad, Hercules, CA, USA).

Sucrose gradients

Sucrose gradients have been prepared as described elsewhere (36). Briefly, 1 mg of protein was loaded onto a 16 ml 10–30% discontinuous sucrose gradient and separated at 22 000× g for 16 h. 24 fractions were collected, and protein was TCA precipitated. Subsequent samples were analyzed via SDS-PAGE.

Immunohistochemistry, fluorescence and electron microscopy

Mitochondrial staining was performed by incubation with Mitotracker CMXRos (ThermoFisher, Waltham, MA, USA) for 15 min in full medium. The medium was replaced, and cells were replaced

in the incubator for 10 min in full medium. Cells were rinsed twice with 1×PBS and fixed in ice-cold acetone for 3 min and mounted in VectaShield (Vector Laboratories, Peterborough, UK). Immunofluorescence microscopy was performed as described before (39). Samples were imaged in a Zeiss Observer 2.1 with ApoTome (Carl Zeiss, Oberkochen, Germany). Image contrast was adjusted within the software of the microscope. Electron microscopy was performed as described before (40). Briefly, cells were grown on 13 mm coverslips, fixed with 2% GA in phosphate buffer, embedded, sectioned and imaged.

Statistical analysis

All statistical analyses and graphs were done using PRISM 7.0ab (GraphPad Software, Inc., La Jolla, CA, USA). Quantifications were performed using either FIJI (ImageJ v.2.0.0) or the western blot chemiluminescence signal intensities using ImageLab 5.2.1 (Biorad, Hercules, CA, USA). Student's *t*-test was used to calculate statistical significances were *P*-values < 0.05 were considered significant ($^{*}P \leq 0.05$, $^{**}P \leq 0.01$. $^{***}P \leq 0.001$).

Supplementary Material

Supplementary Material is available at *HMG* online.

Acknowledgements

We are indebted to the family participating in this study. We thank Tuula Manninen for excellent technical assistance and the Electron microscopy unit of the Institute of Biotechnology and the Functional Genomics (FuGu) center at the University of Helsinki for their services.

Conflict of Interest statement. None declared.

Funding

This work was supported by the Swiss National Science Foundation [to CJ], the Novartis Foundation for medical biological research [to CJ, AS]; the Academy of Finland and Sigrid Jusélius Foundation [to ASu].

References

1. Smits, P., Smeitink, J. and van den Heuvel, L. (2010) Mitochondrial translation and beyond: processes implicated in combined oxidative phosphorylation deficiencies. *J. Biomed. Biotechnol.*, **2010**, 1–24.
2. Kemp, J.P., Smith, P.M., Pyle, A., Neeve, V.C.M., Tuppen, H.A.L., Schara, U., Talim, B., Topaloglu, H., Holinski-Feder, E., Abicht, A. *et al.* (2011) Nuclear factors involved in mitochondrial translation cause a subgroup of combined respiratory chain deficiency. *Brain*, **134**, 183–195.
3. Rötig, A. (2011) Human diseases with impaired mitochondrial protein synthesis. *Biochim. Biophys. Acta*, **1807**, 1198–1205.
4. Amunts, A., Brown, A., Toots, J., Scheres, S.H.W. and Ramakrishnan, V. (2015) Ribosome. The structure of the human mitochondrial ribosome. *Science*, **348**, 95–98.
5. Greber, B.J., Boehringer, D., Leibundgut, M., Bieri, P., Leitner, A., Schmitz, N., Aebersold, R. and Ban, N. (2014) The complete structure of the large subunit of the mammalian mitochondrial ribosome. *Nature*, **515**, 283–286.
6. De Silva, D., Tu, Y.-T., Amunts, A., Fontanesi, F. and Barrientos, A. (2015) Mitochondrial ribosome assembly in health and disease. *Cell Cycle*, **14**, 2226–2250.
7. Greber, B.J. and Ban, N. (2016) Structure and function of the mitochondrial ribosome. *Annu. Rev. Biochem.*, **85**, 103–132.
8. Sharma, M.R., Koc, E.C., Datta, P.P., Booth, T.M., Spremulli, L.L. and Agrawal, R.K. (2003) Structure of the mammalian mitochondrial ribosome reveals an expanded functional role for its component proteins. *Cell*, **115**, 97–108.
9. Ott, M., Amunts, A. and Brown, A. (2016) Organization and regulation of mitochondrial protein synthesis. *Annu. Rev. Biochem.*, **85**, 77–101.
10. Cavdar Koc, E., Burkhart, W., Blackburn, K., Moseley, A. and Spremulli, L.L. (2001) The small subunit of the mammalian mitochondrial ribosome. Identification of the full complement of ribosomal proteins present. *J. Biol. Chem.*, **276**, 19363–19374.
11. Haack, T.B., Jackson, C.B., Murayama, K., Kremer, L.S., Schaller, A., Kotzaeridou, U., de Vries, M.C., Schottmann, G., Santra, S., Büchner, B. *et al.* (2015) Deficiency of ECHS1 causes mitochondrial encephalopathy with cardiac involvement. *Ann. Clin. Transl. Neurol.*, **2**, 492–509, doi:10.1002/acn3.189.
12. Lek, M., Karczewski, K.J., Minikel, E.V., Samocha, K.E., Banks, E., Fennell, T., O'Donnell-Luria, A.H., Ware, J.S., Hill, A.J., Cummings, B.B. *et al.* (2016) Analysis of protein-coding genetic variation in 60,706 humans. *Nature*, **536**, 285–291.
13. Ioannidis, N.M., Rothstein, J.H., Pejaver, V., Middha, S., McDonnell, S.K., Baheti, S., Musolf, A., Li, Q., Holzinger, E., Karyadi, D. *et al.* (2016) REVEL: an ensemble method for predicting the pathogenicity of rare missense variants. *Am. J. Hum. Genet.*, **99**, 877–885.
14. Lake, N.J., Webb, B.D., Stroud, D.A., Richman, T.R., Ruzzenente, B., Compton, A.G., Mountford, H.S., Pulman, J., Zangarelli, C., Rio, M. *et al.* (2017) Biallelic mutations in MRPS34 lead to instability of the small mitoribosomal subunit and Leigh syndrome. *Am. J. Hum. Genet.*, **101**, 239–254.
15. Emdadul Haque, M., Grasso, D., Miller, C., Spremulli, L.L. and Saada, A. (2008) The effect of mutated mitochondrial ribosomal proteins S16 and S22 on the assembly of the small and large ribosomal subunits in human mitochondria. *Mitochondrion*, **8**, 254–261.
16. Serre, V., Rozanska, A., Beinat, M., Chrétien, D., Boddaert, N., Munnich, A., Rötig, A. and Chrzanowska-Lightowlers, Z.M. (2013) Mutations in mitochondrial ribosomal protein MRPL12 leads to growth retardation, neurological deterioration and mitochondrial translation deficiency. *Biochim. Biophys. Acta*, **1832**, 1304–1312.
17. Miller, C., Saada, A., Shaul, N., Shabtai, N., Ben-Shalom, E., Shaag, A., Hershkovitz, E. and Elpeleg, O. (2004) Defective mitochondrial translation caused by a ribosomal protein (MRPS16) mutation. *Ann. Neurol.*, **56**, 734–738.
18. Baertling, F., Haack, T.B., Rodenburg, R.J., Schaper, J., Seibt, A., Strom, T.M., Meitinger, T., Mayatepek, E., Hadzik, B., Selcan, G. *et al.* (2015) MRPS22 mutation causes fatal neonatal lactic acidosis with brain and heart abnormalities. *Neurogenetics*, **16**, 237–240.
19. Menezes, M.J., Guo, Y., Zhang, J., Riley, L.G., Cooper, S.T., Thorburn, D.R., Li, J., Dong, D., Li, Z., Glessner, J. *et al.* (2015) Mutation in mitochondrial ribosomal protein S7 (MRPS7) causes congenital sensorineural deafness, progressive hepatic and renal failure and lactic acidemia. *Hum. Mol. Genet.*, **24**, 2297–2307.

20. Carroll, C.J., Isohanni, P., Pöyhönen, R., Euro, L., Richter, U., Brilhante, V., Götz, A., Lahtinen, T., Paetau, A., Pihko, H. *et al*. (2013) Whole-exome sequencing identifies a mutation in the mitochondrial ribosome protein MRPL44 to underlie mitochondrial infantile cardiomyopathy. *J. Med. Genet*., **50**, 151–159.
21. Bogenhagen, D.F., Ostermeyer-Fay, A.G., Haley, J.D. and Garcia-Diaz, M. (2018) Kinetics and mechanism of mammalian mitochondrial ribosome assembly. *Cell Rep*., **22**, 1935–1944.
22. Kummer, E., Leibundgut, M., Rackham, O., Lee, R.G., Boehringer, D., Filipovska, A. and Ban, N. (2018) Unique features of mammalian mitochondrial translation initiation revealed by cryo-EM. *Nature*, **560**, 263–267.
23. Kaushal, P.S., Sharma, M.R., Booth, T.M., Haque, E.M., Tung, C.-S., Sanbonmatsu, K.Y., Spremulli, L.L. and Agrawal, R.K. (2014) Cryo-EM structure of the small subunit of the mammalian mitochondrial ribosome. *Proc. Natl. Acad. Sci. U. S. A*., **111**, 7284–7289.
24. Galmiche, L., Serre, V., Beinat, M., Assouline, Z., Lebre, A.-S., Chrétien, D., Nietschke, P., Benes, V., Boddaert, N., Sidi, D. *et al*. (2011) Exome sequencing identifies MRPL3 mutation in mitochondrial cardiomyopathy. *Hum. Mutat*., **32**, 1225–1231.
25. Distelmaier, F., Haack, T.B., Catarino, C.B., Gallenmüller, C., Rodenburg, R.J., Strom, T.M., Baertling, F., Meitinger, T., Mayatepek, E., Prokisch, H. *et al*. (2015) MRPL44 mutations cause a slowly progressive multisystem disease with childhood-onset hypertrophic cardiomyopathy. *Neurogenetics*, **16**, 319–323.
26. Gardeitchik, T., Mohamed, M., Ruzzenente, B., Karall, D., Guerrero-Castillo, S., Dalloyaux, D., van den Brand, M., van Kraaij, S., van Asbeck, E., Assouline, Z. *et al*. (2018) Bi-allelic mutations in the mitochondrial ribosomal protein MRPS2 cause sensorineural hearing loss, hypoglycemia, and multiple OXPHOS complex deficiencies. *Am. J. Hum. Genet*., **102**, 685–695.
27. Smits, P., Saada, A., Wortmann, S.B., Heister, A.J., Brink, M., Pfundt, R., Miller, C., Haas, D., Hantschmann, R., Rodenburg, R.J.T. *et al*. (2011) Mutation in mitochondrial ribosomal protein MRPS22 leads to Cornelia de Lange-like phenotype, brain abnormalities and hypertrophic cardiomyopathy. *Eur. J. Hum. Genet*., **19**, 394–399.
28. Saada, A., Shaag, A., Arnon, S., Dolfin, T., Miller, C., Fuchs-Telem, D., Lombès, A. and Elpeleg, O. (2007) Antenatal mitochondrial disease caused by mitochondrial ribosomal protein (MRPS22) mutation. *J. Med. Genet*., **44**, 784–786.
29. Kohda, M., Tokuzawa, Y., Kishita, Y., Nyuzuki, H., Moriyama, Y., Mizuno, Y., Hirata, T., Yatsuka, Y., Yamashita-Sugahara, Y., Nakachi, Y. *et al*. (2016) A comprehensive genomic analysis reveals the genetic landscape of mitochondrial respiratory chain complex deficiencies. *PLoS Genet*., **12**, e1005679–e1005631.
30. Götz, A., Tyynismaa, H., Euro, L., Ellonen, P., Hyötyläinen, T., Ojala, T., Hämäläinen, R.H., Tommiska, J., Raivio, T., Oresic, M. *et al*. (2011) Exome sequencing identifies mitochondrial alanyl-tRNA synthetase mutations in infantile mitochondrial cardiomyopathy. *Am. J. Hum. Genet*., **88**, 635–642.
31. Richter, U., Lahtinen, T., Marttinen, P., Suomi, F. and Battersby, B.J. (2015) Quality control of mitochondrial protein synthesis is required for membrane integrity and cell fitness. *J. Cell Biol*., **211**, 373–389.
32. Berger, T., Brigl, M., Herrmann, J.M., Vielhauer, V., Luckow, B., Schlondorff, D. and Kretzler, M. (2000) The apoptosis mediator mDAP-3 is a novel member of a conserved family of mitochondrial proteins. *J. Cell Sci*., **113**, 3603–3612.
33. Lightowlers, R.N., Rozanska, A. and Chrzanowska-Lightowlers, Z.M. (2014) Mitochondrial protein synthesis: figuring the fundamentals, complexities and complications, of mammalian mitochondrial translation. *FEBS Lett*., **588**, 2496–2503.
34. Yoo, Y.A., Kim, M.J., Park, J.K., Chung, Y.M., Lee, J.H., Chi, S.-G., Kim, J.S. and Yoo, Y.D. (2005) Mitochondrial ribosomal protein L41 suppresses cell growth in association with p 53 and p27Kip1. *Mol. Cell. Biol*., **25**, 6603–6616.
35. Mai, N., Chrzanowska-Lightowlers, Z.M.A. and Lightowlers, R.N. (2017) The process of mammalian mitochondrial protein synthesis. *Cell Tissue Res*., **367**, 5–20.
36. Richter, U., Lahtinen, T., Marttinen, P., Myöhänen, M., Greco, D., Cannino, G., Jacobs, H.T., Lietzén, N., Nyman, T.A. and Battersby, B.J. (2013) A mitochondrial ribosomal and RNA decay pathway blocks cell proliferation. *Curr. Biol*., **23**, 535–541.
37. Jackson, C.B., Nuoffer, J.M., Hahn, D., Prokisch, H., Haberberger, B., Gautschi, M., Haberli, A., Gallati, S. and Schaller, A. (2014) Mutations in SDHD lead to autosomal recessive encephalomyopathy and isolated mitochondrial complex II deficiency. *J. Med. Genet*., **51**, 170–175.
38. Schägger, H. and Jagow, von, G. (1991) Blue native electrophoresis for isolation of membrane protein complexes in enzymatically active form. *Anal. Biochem*., **199**, 223–231.
39. Jackson, C.B., Zbinden, C., Gallati, S. and Schaller, A. (2014) Heterologous expression from the human D-Loop in organello. *Mitochondrion*, **17**, 67–75.
40. Jackson, C.B., Neuwirth, C., Hahn, D., Nuoffer, J.M., Frank, S., Gallati, S. and Schaller, A. (2014) Novel mitochondrial tRNA (Ile) m.4282A>G gene mutation leads to chronic progressive external ophthalmoplegia plus phenotype. *Br. J. Ophthalmol*., **98**, 1453–1459.